EXERCISE 9

Refer to Figure 9.8. If $R = 1$ MΩ and the maximum output of the op-amp is 200 mV, what is the maximum current I?

The output of op-amp 2 is given by

$$V_{\text{out, 2}} = \left(1 + \frac{R_2}{10\text{k}}\right) V_{\text{out, 1}} \qquad \text{(V)} \tag{23}$$

where $V_{\text{out, 1}}$ is the output of op-amp 1.

EXERCISE 10

Assuming that $K = 5$ V and op-amp 1 output ranges from 0 to 200 mV, show that the output of op-amp 2 ranges from 0 to +5 V provided that R_2 is 240 kΩ. (Note only one half of the analog range is utilized. This is because of the need to adjust the output of op-amp 2 to zero when the input to op-amp 1 is the dark current.)

Bench Testing Install the appropriate resistance R_2. In the circuit shown in Figure 9.12, replace the DAC output with the 3-V power supply and 10-kΩ potentiometer shown in Figure 9.8*a*; replace the ADC input with a voltmeter. With the dark current as the input to op-amp 1, set the outputs of 1 and 2 to zero in the order that they are numbered by adjusting the 25-kΩ potentiometer for each op-amp. The potentiometer is shown in Figure 9.8*b*. By using the 546-nm spectral line, say, with the lamp-phototube separation such that the maximum output of op-amp 1 is 200 mV, vary the voltage to the phototube and observe the output of 2. If the circuit functions properly, connect it to the computer as is shown in Figure 9.12.

MEASUREMENTS AND SOFTWARE

Some possible things to do are the following.

1. Write software that increments the DAC output, reads the ADC input for each DAC output, and stores each pair of values.
2. Run the software for each spectral line, and instruct the computer to plot an I-V characteristic curve and to determine the stopping potential.
3. Write software that plots stopping potential versus frequency, analyzes the data, and prints a hard copy.

10. DIFFRACTION OF X RAYS AND MICROWAVES BY PERIODIC STRUCTURES: BRAGG SPECTROSCOPY

Historical Note

The 1914 Nobel prize in Physics was awarded to Max Von Laue, Germany

For his discovery of the diffraction of X-rays by crystals.

The 1915 Nobel prize in Physics was awarded jointly to Sir William Henry Bragg, and his son, Sir William Lawrence Bragg, both of Great Britain

For their serivces in the analysis of crystal structures by means of X-rays.

APPARATUS

X-ray diffractometer system (e.g., Tel-X-Ometer crystallography system, available from PASCO Scientific) which includes:

- Ratemeter or scaler
- Geiger–Mueller (G–M) tube
- Motor drive
- X-ray tube with copper anode
- Scatter shield

NaCl and KCl in powder and single-crystal forms

Ni foil

Microwave Bragg diffraction apparatus (available from Sargent-Welch Scientific Co.) which includes:

- Goniometer
- Cubic lattice of Al spheres in a foam plastic matrix
- Microwave transmitter and receiver

OBJECTIVES

To obtain and analyze single-"crystal" data from the microwave diffraction apparatus as an analog to the Bragg scattering of x rays.

To obtain and analyze x-ray Bragg reflections from single alkali–halide crystals of known orientation.

To obtain and analyze x-ray reflections from a powder sample.

To become acquainted with some aspects of crystal symmetry, particularly as applied to the cubic lattices.

To understand the physical basis of the Bragg reflections from crystal planes as predicted by the Bragg condition and a consideration of the structure factor.

KEY CONCEPTS

Bragg diffraction (scattering)
Bravais lattice
Primitive cell
Basis
Miller indices
Fourier analysis
Reciprocal lattice vector
Structure factor
Form factor
Bremsstrahlung
Characteristic radiation
Absorption edge
Powder (Debye–Scherrer) method

REFERENCES

1. C. Kittel, *Introduction to Solid State Physics*, 6th ed., Wiley, New York, 1985. Chapters 2 and 3 provide a concise, readable introduction to crystal geometry, the reciprocal lattice, and Bragg diffraction.

2. R. Eisberg and R. Resnick, *Quantum Physics of Atoms, Molecules, Solids, Nuclei and Particles*, 2d ed., Wiley, New York, 1985. Section 9 contains a discussion of the production and nomenclature of atomic x-ray emission lines.
3. B. E. Warren, *X-ray Diffraction*, Addison-Wesley, Reading, MA, 1969. Discusses crystal symmetry and diffraction techniques.
4. P. J. Barry and A. D. Brothers, *Am. J. Phys.* **54**, 186 (1986). Describes a technique for interfacing a diffractometer system with a microcomputer for an automated data acquisition system.
5. *International Tables for X-Ray Crystallography*, Vol. 3, Reidel, Boston, 1962. Contains pertinent numerical data such as wavelengths of characteristic x-ray emission lines and absorption edges and atomic form factors.
6. L. V. Azaroff and M. J. Buerger, *The Powder Method in X-Ray Crystallography*, McGraw-Hill, New York, 1958.
7. H. F. Meiners (ed.), *Physics Demonstration Experiments*, Vol. 2, Ronald Press, New York, 1970. The microwave scattering experiment discussed below is based on the arrangement described in Chapter 33, Section 7.15, which features apparatus developed by H. F. Meiners.

INTRODUCTION

When electromagnetic radiation is incident upon a periodic array of scattering centers as in Figure 10.1*a*, there are certain discrete directions for the incident ray that result in strong reflections; this is because of constructive interference of the radiation scattered from each of the centers. The directions for which these strong reflections occur are related through the Bragg law, described in the discussion that follows, to the geometry of the arrangement. Measurements of the angular positions and intensities of these Bragg reflections can be used to deduce the arrangement and spacings of the scatterers. If the scatterers are the atoms or molecules of a crystal of unknown geometry and the radiation is a monochromatic x-ray beam of known wavelength, measurements of the angular distribution and intensities of the reflected beams can be used to determine the crystallographic symmetry and interatomic spacings. Conversely, a crystal with a known structure may be used to spectrally analyze an x-ray beam or as an x-ray monochromator.

X-ray scattering, sometimes referred to as Bragg diffraction, is widely used in research laboratories around the world. One recent estimate puts the number of x-ray diffraction

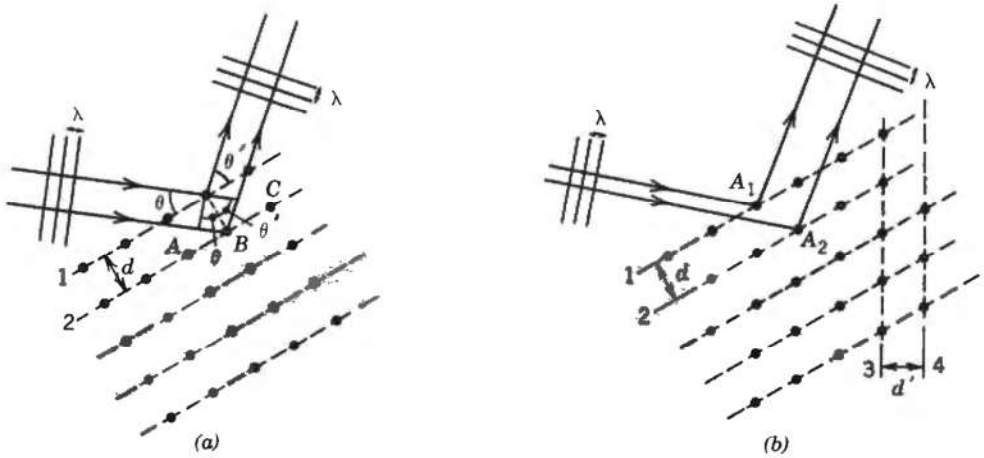

FIGURE 10.1 (*a*) Periodic array of scatterers. (*b*) Periodic array with atoms "misaligned."

users worldwide at about 25 000, one-third of which are in the United States. In addition to basic crystallographic structure analysis, diffraction techniques are also currently useful in such applications as the qualitative and quantitative analysis of material composition, the analysis of stress/strain conditions within a given polycrystalline material, and the study of phase transitions at elevated temperatures. X-ray scattering is also currently being used in the study of macromolecular systems of interest to molecular biologists. Researchers have, for example, studied diffraction patterns from magnetically oriented solutions of macromolecular assemblies that yield subcellular structural information; "movies" of proteins in motion have been produced using high-intensity nanosecond pulses of x rays; the three-dimensional internal structure of complex organic molecules is also currently being probed with x rays.

The analysis of the x-ray diffraction patterns to be observed in this experiment is based on the Bragg law of equation 2, which follows. We derive this law first from a simplified, heuristic, two-dimensional viewpoint, following which is a more general (and somewhat more complex) three-dimensional treatment.

The Bragg Law in Two Dimensions

The Bragg law may be derived in a simple way by considering the reflection (or scattering) of x rays from the planes of atoms indicated in Figure 10.1*a*. If the x rays are treated classically as monochromatic electromagnetic waves of wavelength λ, then the reflections from successive planes of atoms will interfere constructively if the total difference δ in optical path lengths for waves reflected from planes 1 and 2 is an integral number of wavelengths. If the spacing between the indicated planes is d and the incident beam makes an angle θ with these planes, then the path length difference is given by

$$\delta = d(\sin\theta + \sin\theta') \qquad \text{(m)} \tag{1}$$

If we assume that $\theta = \theta'$, as is the case for specular reflection of visible radiation from dielectric or metallic surfaces, then the condition for constructive interference is

$$2d\sin\theta = n\lambda \qquad \text{(m)} \tag{2}$$

where n is a positive integer. Thus, we expect reflections from this family of planes whenever $\theta = \theta'$ and the Bragg law of equation 2 is satisfied.

Note that although we assumed $\theta = \theta'$, this condition emerges as a natural consequence of the requirement that, for a Bragg reflection, atoms within a given plane, as well as atoms in different planes, must scatter constructively. It should also be noted that the Bragg law is a consequence only of the spatial periodicity of the scatterers in a direction perpendicular to the reflecting planes and does not depend on the alignment of the atoms of plane 1 with those of plane 2.

EXERCISE 1

Show that if the Bragg law is satisfied for the situation in Figure 10.1*b*, the radiation scattered from atoms A_1 and A_2 will constructively interfere even though they are not "aligned" in a direction perpendicular to planes 1 and 2 as in Figure 10.1*a*.

Three-Dimensional Description: Bravais Lattices and Miller Indices

The crystalline *lattices* discussed above contain several families of parallel planes in addition to the ones pictured in Figure 10.1*a*, each with its own orientation and spacing (e.g., those parallel to planes 3 and 4 in Figure 10.1*b*), which have the potential to produce Bragg

reflections if equation 2 is satisfied. Additionally, if these lattices are considered as representing an arrangement of scatterers that exhibits periodicity in each of three dimensions, the enumeration of all the possible reflections from every family of planes is a formidable task that requires an understanding of the geometry of crystals in three dimensions.

The structure of a crystalline arrangement of atoms or molecules is described by specifying a basic repetitive unit of the lattice, the unit cell. The fourteen fundamental types of three-dimensional crystal lattices, the so-called Bravais lattices, are divided into seven crystal systems according to the geometry of the unit cell; these are listed in Table 10.1. Figure 10.2*a* shows the cell geometry and location of the lattice points for each cell. The choice of unit cell for each type of lattice is not unique; the cells shown here are the conventional ones rather than the "primitive" cells of minimum volume. Each cell is described conveniently in terms of a set of axes and three translation vectors $\mathbf{a}_1$, $\mathbf{a}_2$, and $\mathbf{a}_3$, as pictured in Figure 10.2*b*. The restrictions on the angles α, β, and γ are given in the third column of Table 10.1. The relationship between the translation vectors, the unit cell, and the structure of the crystal is illustrated by Figure 10.2*c*. As can be seen here, a cell can be translated into any other cell in the lattice by a displacement of the form $l\mathbf{a}_1 + m\mathbf{a}_2 + n\mathbf{a}_3$, where l, m, and n are integers. To complete the specification of the crystal structure it is necessary to specify a basis, that is, a group of atoms or molecules to be associated with each point of the lattice.

Of particular interest in this experiment is the cubic system with its three lattice types shown in the top row of Figure 10.2: simple cubic (sc), body-centered cubic (bcc), and face-centered cubic (fcc). The unit cell for all three structures is a cube, but the location of the lattice points within the cube differs for each structure. The NaCl crystal, an important example of a crystal structure with an fcc lattice, can be described by choosing a basis consisting of one Na^+ ion and one Cl^- ion. If an Na^+ ion is considered to be located at each fcc lattice point, then a Cl^- ion is found displaced by a vector $\frac{1}{2}\mathbf{a}_1 + \frac{1}{2}\mathbf{a}_2 + \frac{1}{2}\mathbf{a}_3$ with

TABLE 10.1 THE SEVEN CRYSTAL SYSTEMS

System	*Number of Lattices*	*Restrictions on Conventional Cell Axes and Angles*
Triclinic	1	$a_1 \neq a_2 \neq a_3$ $\alpha \neq \beta \neq \gamma$
Monoclinic	2	$a_1 \neq a_2 \neq a_3$ $\alpha = \gamma = 90° \neq \beta$
Orthorhombic	4	$a_1 \neq a_2 \neq a_3$ $\alpha = \beta = \gamma = 90°$
Tetragonal	2	$a_1 = a_2 \neq a_3$ $\alpha = \beta = \gamma = 90°$
Cubic	3	$a_1 = a_2 = a_3$ $\alpha = \beta = \gamma = 90°$
Trigonal	1	$a_1 = a_2 = a_3$ $\alpha = \beta = \gamma < 120°, \neq 90°$
Hexagonal	1	$a_1 = a_2 \neq a_3$ $\alpha = \beta = 90°$ $\gamma = 120°$

Source: C. Kittel, *Introduction to Solid State Physics*, Sixth Edition, Wiley, New York, 1986. Copyright © 1986, John Wiley & Sons, Inc. Reprinted by permission.

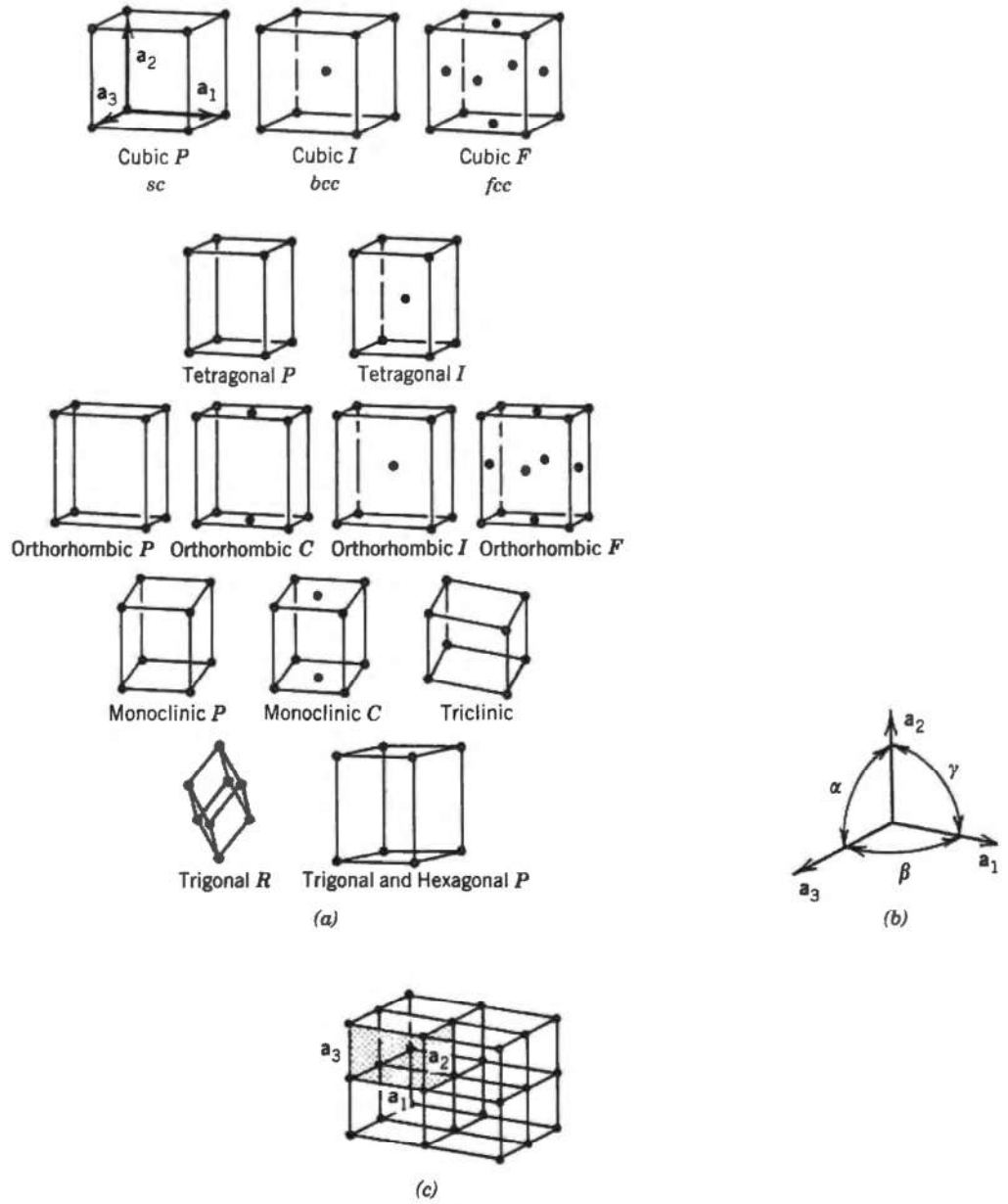

FIGURE 10.2 (*a*) Cell geometry for the Bravais lattices. (*b*) Translation vectors for the unit cell. (*c*) Relationship between the unit cell, the translation vectors, and the crystal structure.

respect to each Na^+, where $|\mathbf{a}_1| = |\mathbf{a}_2| = |\mathbf{a}_3| = a$, the length of the side of the unit cube. This arrangement is shown in Figure 10.3.

The standard way to specify the three-dimensional orientation of the planes of scatterers associated with each possible Bragg reflection is by use of Miller indices. The Miller indices specifying a plane such as the one depicted in Figure 10.4*a* is a set of three numbers (*hkl*) determined from the intercepts of the plane on the three crystal axes. To find the indices for a plane: (1) find the intercepts along each axis, expressed in units of the translation vector parallel to that axis; (2) take the reciprocal of each of these three numbers; (3) multiply each of the three numbers by the smallest integer necessary to clear the fractions. For the plane of Figure 10.4*a*, the intercepts are expressed in ordered triplet form as (322), from which the reciprocals are $(\frac{1}{3}, \frac{1}{2}, \frac{1}{2})$. Clearing fractions gives (233) as the Miller indices of this family of planes.

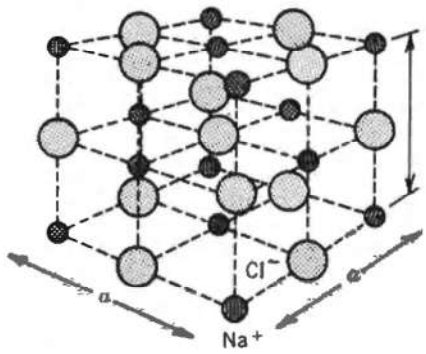

FIGURE 10.3 The structure of an NaCl crystal.

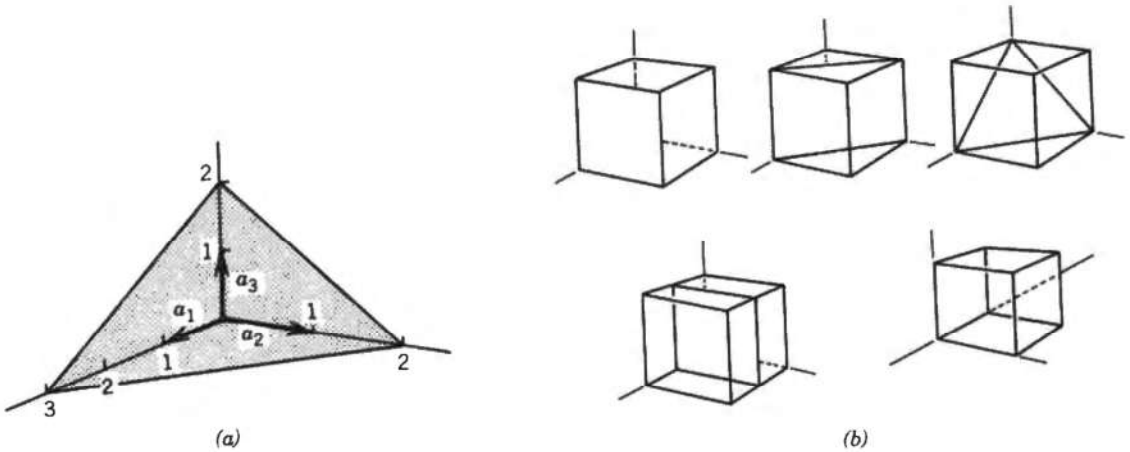

FIGURE 10.4 (*a*) Crystal plane shown with intercepts on axes. (*b*) Various planes within cubic unit cell.

EXERCISE 2

Determine the Miller indices for each of the planes shown with the cubic unit cell in Figure 10.4*b*. Note that for negative digits in a set of indices, minus signs are conventionally written as dashes above the digit, for example, $(1, \bar{1}, 0)$.

Bragg Diffraction in Three Dimensions; Reciprocal Lattice Vectors

To predict the directions in which x rays will be Bragg reflected from a crystal of given geometry, consider the situation of Figure 10.5, in which the x-ray source emits a plane wave with wave vector $\mathbf{k}$ ($k = 2\pi/\lambda$) of the form

$$\mathbf{E}_i = \mathbf{E}_{0i}\, e^{j(\mathbf{k}\cdot\mathbf{r} - \omega t)} \qquad \text{(N/C)} \tag{3}$$

which is incident upon the volume element of crystal dV located at $\mathbf{r}$ with respect to an origin O. The electrons within this element respond to the wave by scattering radiation which, at the detector, has an amplitude proportional to

$$E_i\, e^{j[\mathbf{k}'\cdot(\mathbf{r}_D - \mathbf{r})]}\, n(\mathbf{r})\, dV \qquad \text{(N/C)} \tag{4}$$

where $n(\mathbf{r})$ is the electron density in dV and $\mathbf{k}'$ is the wave vector of the scattered wave.

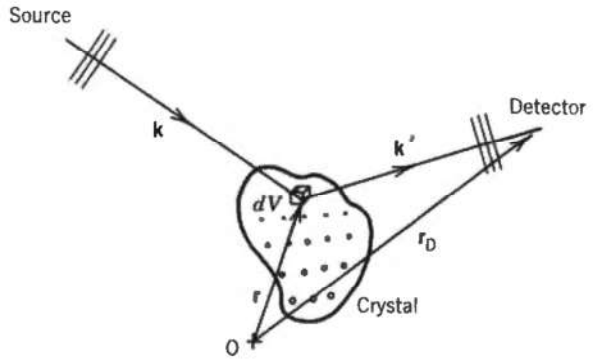

FIGURE 10.5 X-ray plane wave scattered from a volume element of a crystal.

Ignoring both the time dependence and the constant phase $\mathbf{k}' \cdot \mathbf{r}_D$, the behavior of the amplitude of the scattered wave E_s at the detector is given by

$$E_s \propto n(\mathbf{r})\, e^{j[(\mathbf{k}-\mathbf{k}')\cdot\mathbf{r}]}\, dV \tag{5}$$

The amplitude of the radiation at the detector due to scattering by the entire crystal is proportional to a quantity obtained by performing a volume integral of equation 5 over the electron distribution of the crystal. The result is the scattering amplitude F:

$$F = \int dV\, n(\mathbf{r})\, e^{-j[\Delta\mathbf{k}\cdot\mathbf{r}]} \tag{6}$$

where $\Delta\mathbf{k} \equiv \mathbf{k}' - \mathbf{k}$ is called the scattering vector. To obtain from equation 6 the values of Δk for which there will be strong Bragg reflections, it is necessary to Fourier analyze the electron density function $n(\mathbf{r})$. This is done by writing $n(\mathbf{r})$ as a sum:

$$n(\mathbf{r}) = \sum_{\mathbf{G}} n_{\mathbf{G}}\, e^{j(\mathbf{G}\cdot\mathbf{r})} \qquad (\mathrm{m}^{-3}) \tag{7}$$

where the $n_{\mathbf{G}}$ values are possibly complex and the summation ranges over all possible reciprocal lattice vectors $\mathbf{G}$, which we now define as

$$\mathbf{G}(hkl) = h\mathbf{b}_1 + k\mathbf{b}_2 + l\mathbf{b}_3 \qquad (\mathrm{m}^{-1}) \tag{8}$$

Each combination of integers (hkl) specifies a different $\mathbf{G}$. The vectors $\mathbf{b}_1$, $\mathbf{b}_2$, and $\mathbf{b}_3$ constitute a basis for the *reciprocal lattice* and are defined in terms of the crystal translation vectors

$$\mathbf{b}_1 = 2\pi \frac{\mathbf{a}_2 \times \mathbf{a}_3}{\mathbf{a}_1 \cdot \mathbf{a}_2 \times \mathbf{a}_3} \qquad \mathbf{b}_2 = 2\pi \frac{\mathbf{a}_3 \times \mathbf{a}_1}{\mathbf{a}_1 \cdot \mathbf{a}_2 \times \mathbf{a}_3} \qquad \mathbf{b}_3 = 2\pi \frac{\mathbf{a}_1 \times \mathbf{a}_2}{\mathbf{a}_1 \cdot \mathbf{a}_2 \times \mathbf{a}_3} \qquad (\mathrm{m}^{-1}) \tag{9}$$

EXERCISE 3

Calculate the reciprocal lattice vectors $\mathbf{G}$ for a simple cubic lattice of side a. Verify that the expansion of equation 7 for the function $n(\mathbf{r})$, which repeats in each unit cell of Figure 10.2*c*, is simply the three-dimensional Fourier series representation of this function.

EXERCISE 4

Show that, for the vectors $\mathbf{b}_1$, $\mathbf{b}_2$, and $\mathbf{b}_3$ defined above, $a_i \cdot b_j = 2\pi\delta_{ij}$. Use this orthogonality relationship to show that each reciprocal lattice vector $\mathbf{G}(hkl)$ is perpendicular to the set of planes with Miller indices (hkl).

EXERCISE 5

Use the result of Exercise 4 to show that the spacing between planes (hkl) is given by $d(hkl) = 2\pi/|G(hkl)|$. Calculate $d(hkl)$ for a cubic lattice of side a.

We can invert the sum in equation 7 by the standard procedures of Fourier analysis to obtain an expression for $n_{\mathbf{G}}$, the Fourier coefficient corresponding to $\mathbf{G}$:

$$n_{\mathbf{G}} = V_C^{-1} \int_{\text{cell}} dV\, n(\mathbf{r})\, e^{-j(\mathbf{G}\cdot\mathbf{r})} \qquad (\text{m}^{-3}) \tag{10}$$

where V_C is the volume of the unit cell over which the integral is to be done.

Using the expansion of equation 7 for $n(\mathbf{r})$ in the expression for the scattering amplitude F of equation 6 gives us a useful form for F:

$$F = \sum_{\mathbf{G}} \int_{\text{crystal}} dV\, n_{\mathbf{G}}\, e^{j[(\mathbf{G}-\Delta\mathbf{k})\cdot\mathbf{r}]} \tag{11}$$

Each term in the above sum contains an exponential which, if its argument is nonzero, oscillates in such a way that integrating over the crystal volume gives zero for that term. Thus, the only way F can be nonzero, so that a reflection can occur, is if the scattering vector $\Delta\mathbf{k}$ happens to equal one of the $\mathbf{G}$ values, making the exponential equal to unity for one term of the sum. Hence, a necessary condition on $\Delta\mathbf{k}$ $(=\mathbf{k}' - \mathbf{k})$ for the occurrence of a Bragg reflection is

$$\Delta\mathbf{k} = \mathbf{G} \qquad (\text{m}^{-1}) \tag{12}$$

where $\mathbf{G}$ is any of the reciprocal lattice vectors defined by equation 8. If we limit our

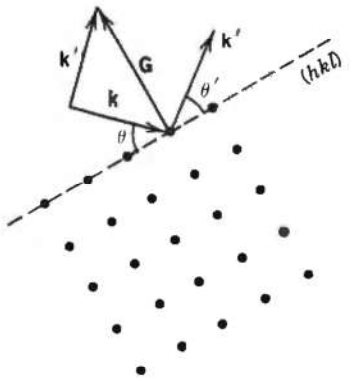

FIGURE 10.6 Initial wave vector, final wave vector, and the scattering vector for a Bragg reflection.

consideration to elastic (coherent) scattering in which the wavelength is unaltered, we have the additional restriction

$$\mathbf{k}' = \mathbf{k} \qquad (\mathrm{m}^{-1}) \tag{13}$$

An example of a Bragg reflection satisfying the conditions of equations 12 and 13 is illustrated in Figure 10.6, where **G**, the scattering vector for this reflection, is drawn perpendicular to the reflecting plane (*hkl*).

EXERCISE 6

Verify with the aid of Figure 10.6 that the two conditions for Bragg reflection cited above imply $\theta = \theta'$.

It is straightforward to show that the conditions expressed by equations 12 and 13 for Bragg reflections imply the two-dimensional form of the specular reflection law of equation 2. Rewriting equation 12 as

$$\mathbf{k}' = \mathbf{k} + \mathbf{G} \qquad (\mathrm{m}^{-1}) \tag{14}$$

and taking the squared magnitude of both sides gives

$$k'^2 = k^2 + G^2 + 2\mathbf{k} \cdot \mathbf{G} \qquad (\mathrm{m}^{-2}) \tag{15}$$

Applying the condition of equation 13 and writing (with reference to Figure 10.6) $\mathbf{k} \cdot \mathbf{G}$ as $-kG \sin\theta$ gives

$$2k \sin\theta = G \qquad (\mathrm{m}^{-1}) \tag{16}$$

Recall that **G** can be any reciprocal lattice vector that is (according to the result of Exercise 4) perpendicular to the plane (*hkl*) doing the reflecting, so that $\mathbf{G} = n\mathbf{G}(hkl)$, where n is any integer. Using the result of Exercise 5, we have

$$\frac{2\pi}{d(hkl)} = G(hkl) = \frac{G}{n} \qquad (\mathrm{m}^{-1}) \tag{17}$$

for the relationship between $d(hkl)$ and G. Using this to eliminate G in equation 16 and inserting the definition of the wave vector **k** yields the Bragg law

$$2\,d(hkl) \sin\theta = n\lambda \qquad (\mathrm{m}) \tag{18}$$

as in equation 2 above.

The preceding discussion of the space and reciprocal lattices and their relationship to the scattering amplitude not only yields a more general interpretation of the Bragg law, as derived in a simple way from Figure 10.1, but also gives us information with regard to the expected intensities of the reflections from different sets of planes (*hkl*). In particular, the conditions cited above for Bragg reflections are necessary but not sufficient, and some of the reflections permitted by equation 18 will be absent because of the possibility of destructive interference between waves scattered by atoms in the same cell. The discussion of this feature of Bragg reflection requires a further examination of the scattering amplitude of equation 11 and a brief discussion of form and structure factors.

Structure Factor and Form Factor

If equation 12 is satisfied so that for some **G**, $\Delta\mathbf{k} = \mathbf{G}$, then the exponential appearing in the expression for the scattering amplitude F in equation 11 is just unity, and F (denoted by $F_\mathbf{G}$ for this particular **G**) is then given by

$$F_\mathbf{G} = \int n_\mathbf{G}\, dV \tag{19}$$

where the integration is performed over the entire volume of the crystal. Substituting for $n_\mathbf{G}$, the Fourier coefficient of $n(\mathbf{r})$ given by equation 10, gives an expression for the scattering amplitude in terms of the electron distribution within a single cell:

$$F_\mathbf{G} = N\left[\int_{\text{cell}} dV\, n(\mathbf{r})\, e^{-j(\mathbf{G}\cdot\mathbf{r})}\right] \tag{20}$$

where N is the number of cells in the crystal and the expression within the square brackets is called the structure factor $S_\mathbf{G}$. The electron density function $n(\mathbf{r})$ is often most conveniently broken up into chunks associated with each of the atoms contained within the cell, which is the region of integration in equation 20. If this is done, then this integral can be expressed as a simple sum:

$$F_\mathbf{G} = NS_\mathbf{G} = N\left[\sum_i f_i\, e^{-j(\mathbf{G}\cdot\mathbf{r}_i)}\right] \tag{21}$$

in which the f_i are known as form factors for the atoms and the sum is over all atoms in the cell located at positions $\mathbf{r}_i$; each f_i is effectively a portion of the integral in equation 20 over the charge distribution associated with the ith atom. The value of $F_\mathbf{G}$, for any $G(hkl)$, determines whether there will be a reflection corresponding to the atomic plane (hkl) and, hence, to $\Delta\mathbf{k} = \mathbf{G}(hkl)$.

EXERCISE 7

Using the conventional cubic cell, calculate $\mathbf{G}(hkl)$ from the definitions of equations 8 and 9. Evaluate $S_\mathbf{G}$ for the fcc lattice of single atoms, assuming identical form factors f_i for all atoms. Note that each conventional cell in the fcc lattice contains four atoms, so that $S_\mathbf{G}$ will contain four terms. You should show that if h, k, and l are either all even or all odd, then the structure factor for $\mathbf{G}(hkl)$ will be nonzero, but that for other combinations of the indices, $S_\mathbf{G}$ will be zero. Reflections from a plane (hkl) that are permitted by the Bragg law but for which the structure factor corresponding to $\mathbf{G}(hkl)$ is zero will not be detected.

EXERCISE 8

KCl has the structure shown in Figure 10.3. The lattice is fcc with a basis consisting of one K atom and one Cl atom; one pair of atoms is associated with each lattice site. Because K^+ and Cl^- have the same number of electrons, their form factors f are nearly equal and so they appear as identical ions to an x-ray beam. Calculate the structure factors $S_\mathbf{G}$ for this crystal, keeping in mind that each unit cell now contains 8 ions. What additional restrictions are placed on planes (hkl) that can produce Bragg reflections over and above those for a general monatomic fcc lattice considered in Exercise 7? Can you give a physical explanation for the additional reflections that are now absent?

Production of X Rays

In this set of experiments Bragg diffraction of both x rays and microwaves from periodic structures will be studied. The production of microwaves is discussed in connection with Experiment 2; here we give a brief account of the production the x rays we will use.

Figure 10.7*a* is a schematic representation of an x-ray tube. Electrons are emitted thermionically from the heated cathode, which is maintained at a large potential difference V with respect to the anode target. As these electrons impact the anode, x rays are emitted with a spectral intensity distribution similar to the one shown in Figure 10.7*b*. This spectrum exhibits two main features:

(1) There is a broad continuous spectrum of radiation, referred to as **bremsstrahlung**, caused by the sudden deceleration of the electrons as they impact the anode. (The word is derived from the German words *brems* (braking) and *strahlung* (radiation).) This radiation extends spectrally out to long wavelengths (low photon energies) with decreasing intensity and down to a minimum wavelength $\lambda_0 = hc/Ve$, which is the wavelength of a photon that carries away all the kinetic energy of an electron incident on the anode. From the point of view of x-ray diffraction, this component of the tube emission is often considered as background.

(2) Superimposed on the *bremsstrahlung* continuum is the nearly monochromatic set of

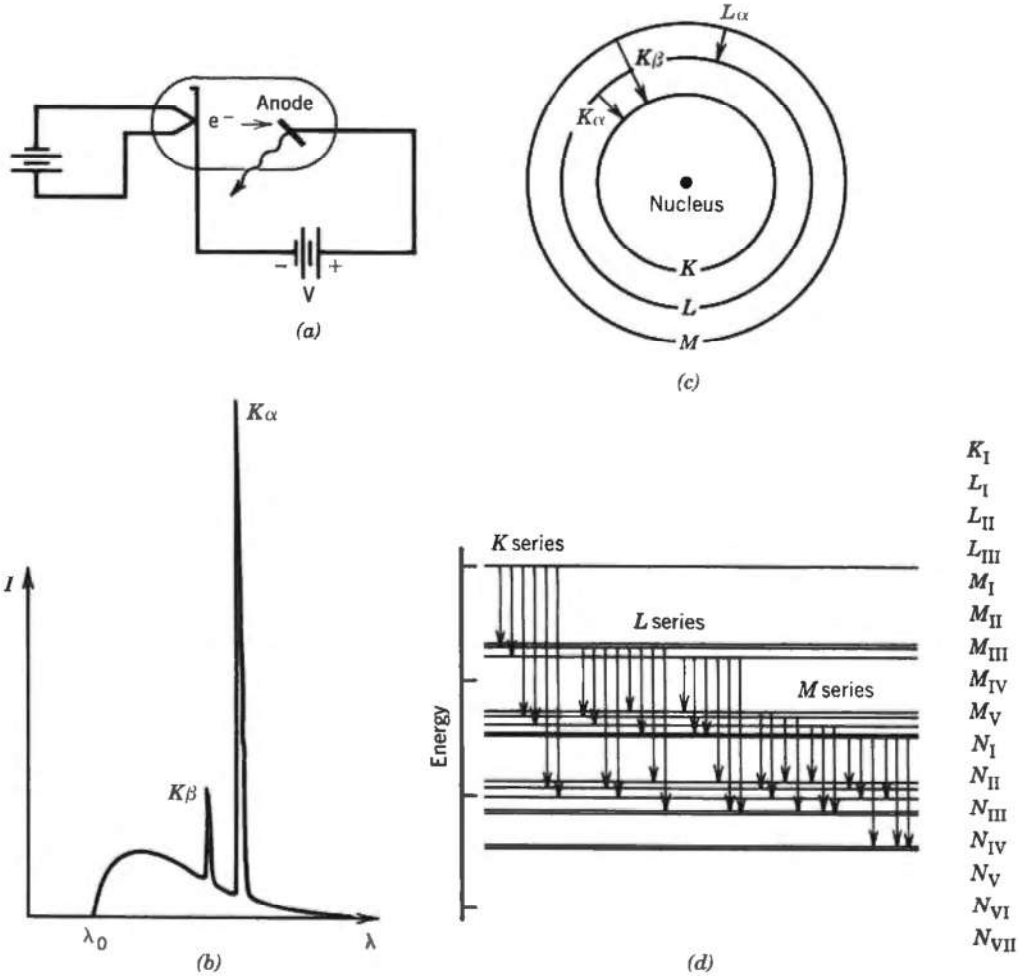

FIGURE 10.7 (*a*) Production of x rays. (*b*) Typical spectral intensity distribution of the output of an x-ray tube. (*c*) Atomic transitions associated with the production of characteristic radiation. (*d*) Energy-level diagram for a vacancy (hole) and the allowed x-ray transitions.

x-ray lines that reflect the atomic structure of the atoms of the anode. The mechanism for the production of this **characteristic radiation** is suggested by Figure 10.7*c*. A high-energy electron impacts the anode and knocks out an inner shell electron from an anode atom. An x-ray photon is emitted when the vacancy thus created is filled by means of a downward transition made by an electron in one of the higher energy shells. The process can be represented on an energy diagram like that of Figure 10.7*d*, which represents the energy of an atom with a vacancy in a particular shell along with transitions allowed by the selection rules. The nomenclature for the various lines is derived from the initial and final states of the transition, as is suggested by Figure 10.7*c*. Note that the spin–orbit interaction, along with other relativistic effects, creates a splitting of the energy levels of the various shells according to the quantum number j, which indexes the total angular momentum. The line K_α, for example, is really a multiplet consisting of two lines (K_{α_1}, K_{α_2}), which are seldom resolved in x-ray diffraction work.

Because of its monochromatic nature, the characteristic radiation described above is quite useful for x-ray diffraction. In this experiment you will use an anode made of Cu, for which the important emission lines are K_α ($\lambda = 0.154178$ nm) and K_β ($\lambda = 0.139217$ nm). The wavelength given for the K_α radiation is a weighted average for the doublet $K_{\alpha_{1,2}}$. The K_β radiation from Cu is about six times weaker than the K_α so that diffraction patterns can be made easier to interpret if the K_β is selectively filtered out. This can be done conveniently for Cu K radiation by means of a foil made of Ni, which has an absorption *edge* (due to photoelectric absorption) at $\lambda = 0.148802$ nm, so that wavelengths shorter than this are selectively absorbed. A Ni foil with a "thickness" of 19 mg/cm, for example, when used as a filter for Cu K, will produce a beam with a K_α component that is 500 times more intense than the K_β.

EXPERIMENT

Microwave Bragg Diffraction

This part of the experiment is an investigation of scattering of microwaves with $\lambda \cong 3$ cm from a cubic lattice of aluminum spheres as an analog to the diffraction of x rays from a crystalline substance. The principles of operation of the reflex klystron and the diode detector are discussed in connection with Experiment 2.

(a) *Wavelength Measurement.* After an appropriate warm-up period and with the klystron transmitter and diode receiver configured as in Figure 10.8*a*, adjust the repeller voltage on the klystron for a peak reading on the receiver meter. With the units arranged as in Figure 10.8*b* in front of a sheet of aluminum (about 30 × 30 cm), move the receiver along the meter stick and observe maxima (antinodes) and minima (nodes) in the standing-wave pattern produced by reflection from the sheet. Obtain the best value for the separation between nodes by measuring the distance through which the receiver travels in producing some large number of these peaks and dips in the signal. Repeat this measurement a few times.

EXERCISE 9

How is the distance between nodes obtained above related to the wavelength of the microwaves? Report the best value of λ, along with an estimate of the uncertainty.

If the apparatus for Experiment 2 is available, you can make a precision measurement of λ with the wavemeter as an alternative to the technique described above.

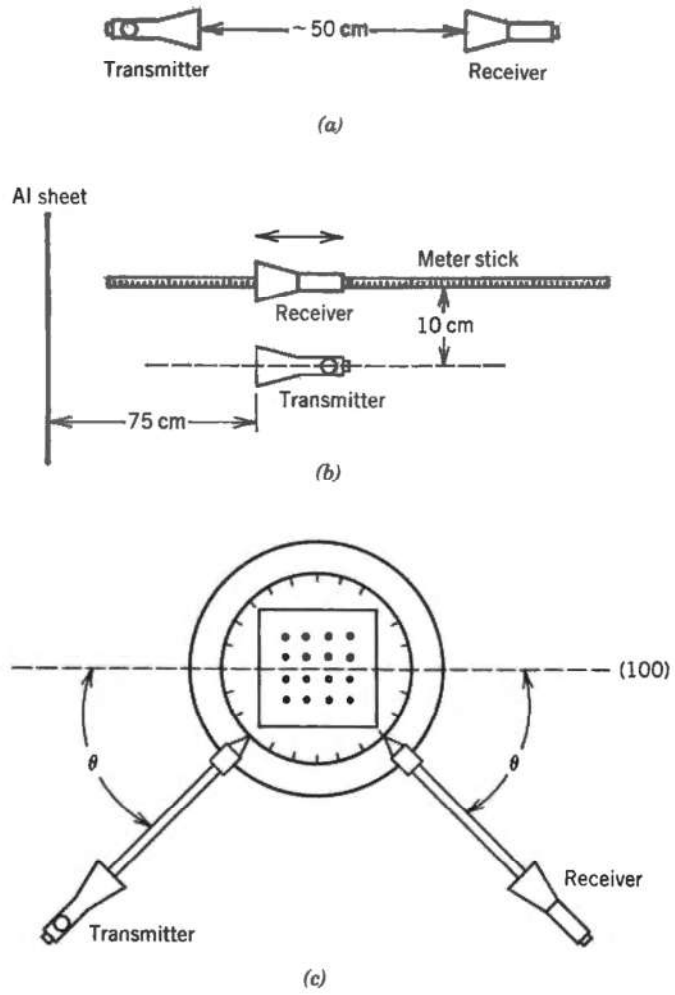

FIGURE 10.8 (*a*) Klystron transmitter and diode receiver.
(*b*) Configuration for wavelength measurement.
(*c*) Configuration for scattering measurement.

(b) *Bragg Reflection from a "Crystal."* Align the layers of Styrofoam with the Al balls so that a cubic arrangement of scatterers is formed. Peak the transmitter output as in (a) and arrange the transmitter, receiver and crystal on the goniometer as in Figure 10.8*c* so that reflections off the (100) plane of scatterers can be measured. Record readings from the receiver as θ is varied in 1° increments. Note that both receiver and transmitter positions must be changed between readings to keep the angles of reflection and incidence equal. Make an intensity versus θ plot.

EXERCISE 10

From your data, calculate the spacing between (100) planes in the crystal. Compare this with a direct measurement of the side of the unit cube.

EXERCISE 11

As stated in connection with Exercise 4, the reciprocal lattice vectors $G(hkl)$ are perpendicular to the planes (hkl). Use this fact to calculate the angle between the (100) planes and

those with indices (110) and (210). Also, use the expression given in Exercise 5 for $d(hkl)$ to calculate the spacing between these two additional sets of planes in terms of the (100) spacings.

Use the angles calculated above to rotate the crystal so that reflection data can be taken for the (100) and (210) planes. Collect, plot, and analyze this data to deduce experimental values for the interplanar spacings. Compare these to the spacings calculated from the result of Exercise 11 by using the directly measured (100) spacings.

X-Ray Bragg Diffraction

Note: As with all ionizing radiation, caution should be exercised to avoid unnecessary bodily exposure. A scattering shield (standard equipment on the Tel-X-Ometer) should be in place when the x-ray tube is in operation.

(a) *Single Crystal.* Mount the NaCl single crystal in the crystal mount of the diffractometer arrangement so that the (100) face is parallel to the back of mount, as shown schematically in Figure 10.9. Use an accelerating voltage of 30 kV for the x-ray tube and a current consistent with its power rating to produce a collimated beam of x rays that strikes the crystal face as shown. The diffractometer should be in θ–2θ mode, that is, the G–M detector arm should move through an angle 2θ whenever the crystal holder turns through θ so that the angles of incidence and reflection remain equal as the angle θ is scanned.

For values of θ within the range of motion of the diffractometer, record the detected intensity versus θ. Plot the data.

Repeat the scan with the Ni foil in the incident x-ray beam.

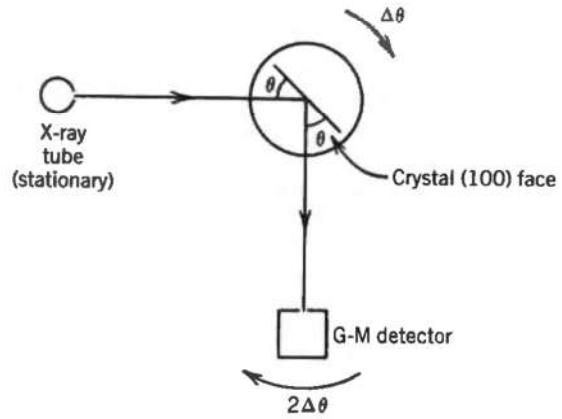

FIGURE 10.9 Arrangement for measurement of single-crystal diffraction.

EXERCISE 12

Identify each observed peak with respect to the value of n (the order) in the Bragg condition of equation 18 and with respect to the wavelength of the radiation responsible for it. Tabulate the angular positions of the peaks and, from the known wavelengths involved, calculate values for $d(100)$ in NaCl. You should keep in mind the restrictions that the discussion of Exercises 7 and 8 place on the reflections. For NaCl the edge of the unit cube of Figure 10.3 has an accepted length of $a = 0.563$ nm. How does this compare with the best value derived from your data?

Repeat the measurements and analysis for the (100) face of a KCl single crystal, for which the accepted value of a is 0.629 nm. Account for the differences in the KCl and NaCl patterns.

(b) *Powder (Debye–Scherrer) Method.* In a powder sample composed of a large number of small crystallites with random orientation, each set of planes (hkl) exhibits all possible orientations with respect to the incident x-ray beam, as depicted in Figure 10.10*a*. The Bragg condition of equation 18 for each set of indices (hkl) is thus always satisfied for some small fraction of the crystallites. This means that, for each set of planes associated with a nonzero structure factor, we expect a specular reflection at the Bragg angle with respect to these planes, that is, at an angle 2θ with respect to the direction of the incident beam. The locus of all such directions is a set of cones with half-angles 2θ and with the incident beam direction as a common axis, as shown in Figure 10.10*b*.

If a cylindrical band of photographic film is positioned with its diameter coincident with the incident beam, the Bragg angles may be determined by measuring the angular positions of the exposed rings. In this arrangement, known as a **powder camera**, the sample should be a powder formed into a cylinder perpendicular to the plane of the film so that all reflections can be recorded photographically.

If a powder camera is unavailable, the angular positions of the Bragg reflections may be determined by scanning the G–M tube position while keeping the sample and x-ray tube stationary, as suggested by Figure 10.10*a*. The sample can be prepared by grinding the substance to a fine powder with a ceramic mortar and pestle and allowing it to stand until enough moisture has been absorbed from the air so that it can be conveniently packed onto a glass microscope slide.

Obtain the angular positions of the powder peaks for NaCl and KCl as discussed above. For each peak, tabulate the Bragg angle θ, $d(hkl)$, and the quantity $m^2d^2(hkl)$, where m^2 takes on all integer values up to 20.

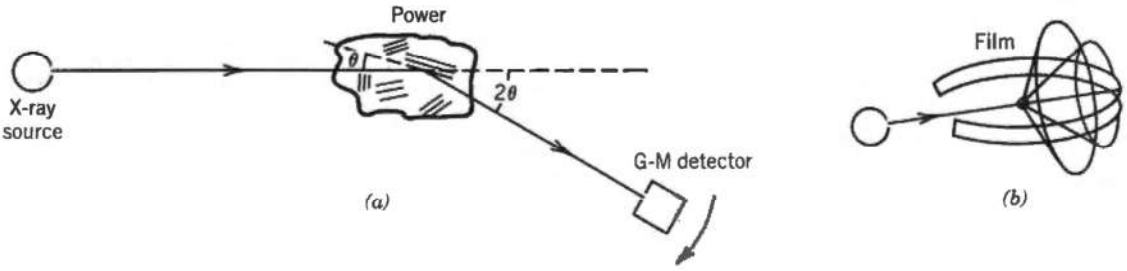

FIGURE 10.10 (*a*) Diffraction from a powder sample. (*b*) Locus of diffraction angles in a powder camera.

EXERCISE 13

From your tabulation and the relation between $d(hkl)$ and the cubic cell side a (see Exercise 5), identify, for each peak, the entry in your tabulation which corresponds to the common value of a. Assign Miller indices (hkl) to each peak reflection.

EXERCISE 14

Determine the best value of a for NaCl and KCl. How do these compare with the accepted values given above? You may wish to weight your average, keeping in mind that smaller values of the measured angles 2θ are likely to contain larger relative errors.

COMPUTER-ASSISTED EXPERIMENTATION (OPTIONAL)

Prerequisite

Experiment 6, Introduction to Computer-Assisted Experimentation.

Experiment

A complete computer interface for an x-ray Bragg spectrometer should consist of (a) a means of acquiring a count rate from a detector, (b) a means of recording the angular position of the detector arm, (c) a mechanism by which the computer can increment the angular position of the detector arm and/or crystal mount between readings (if possible for a particular system), and (d) software instructions to plot the data so that peak positions may be obtained. We discuss the details for implementing (a) and (b) below.

(a) The conditioning circuit shown in Figure 6.11*a* is suitable for counting pulses input from a G–M tube to a scaler/timer. Figure 6.11*b* shows the output of each stage of the conditioning circuit, which finally presents, for each input pulse, a digital pulse to the analog input of the ADC. The text of Experiment 6 contains a thorough discussion of the details of this circuit.

(b) One possibility for recording the angular position of the detector arm is discussed in reference 4 for the Tel-X-Ometer unit in particular. A miniature 10-turn, 10-kΩ potentiometer is configured as a voltage divider as indicated in Figure 10.11 and the center lead is connected to the input of the ADC card, so that the angular position of its shaft is digitized. The potentiometer is mounted in a bracket attached to the thumbwheel on the detector arm; its shaft is then mechanically coupled, by means of a small section of rubber tubing, to the end of a metal shaft that is installed coaxially with the thumbwheel. As the detector arm is taken through a Bragg angle range of 100°, the thumbwheel and potentiometer shafts complete about nine revolutions. For maximum angular resolution, the dc voltages V_1 and V_2 should be adjusted so that taking the detector through the angular range of interest will cause the input of the ADC to traverse the entire allowable range.

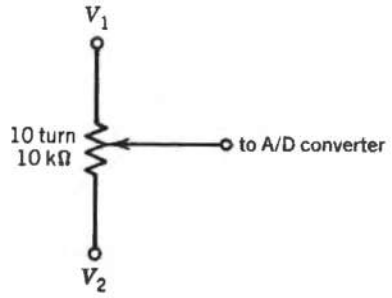

FIGURE 10.11 Voltage divider for digitizing the angular position of the detector.

EXERCISE 15

Determine, for your A/D card, optimal values of V_1 and V_2 if data are to be taken over the range $10° < \theta < 110°$. From the number of bits in your card's digital output, determine the angular resolution of the system for this range of Bragg angles. How does this compare with the uncertainty in the angle readings taken from the scale of the spectrometer?

Measurements and Software

Software needs to convert each potentiometer voltage to an angle, acquire the number of pulses received for each position during some fixed counting period, store the data, and plot the results.

Calibration should be achieved at the beginning of each run by setting the detector at the end points of the range. Background counts need to be acquired and used to adjust the data. The maximum allowable count rate will be determined by the G–M tube and by the software. This last consideration is discussed further in the text of Experiment 6, in the section entitled Computer-Assisted Counting and Data Analysis.

Atomic and Molecular Physics

11. FRANCK–HERTZ EXPERIMENT: ELECTRON SPECTROSCOPY

Historical Note

The 1925 Nobel prize in Physics was awarded jointly to James Franck, Germany and Gustav Hertz, Germany

For their discovery of the laws governing the impact of an electron upon an atom

Franck and Hertz performed the experiment in 1914, 12 years before the development of quantum mechanics, and it provided striking evidence that atomic energy states are quantized.

APPARATUS [Optional Apparatus in brackets]

Franck–Hertz tube
Electric oven
Variac
Thermocouple and temperature potentiometer
Electrometer
Circuit to provide dc voltages for the Franck–Hertz tube, see Figure 11.5
6.3-V ac filament supply
Oscilloscope [with an available sawtooth voltage]